The scale of the diffraction pattern from IPS to understand the evolution of small-scale density fluctuations in the solar wind

Julio Mejia-Ambriz[1], E. Aguilar-Rodriguez[2] , J.A. Gonzalez-Esparza[2] , P. Villanueva-Hernandez[2], E. Andrade-Mascote[2] , A. Espinosa-Jimenez[2] , J.L. Godoy [2]

[1]CONACyT, Laboratorio Nacional de Clima Espacial (LANCE), Instituto de Geofísica, UNAM
[2] LANCE, Instituto de Geofísica, UNAM

Scintillating Science: Cutting-Edge Science Achieved Through the Observations of Radio Scintillation

July 2019

MEXART

The Mexican Array Radio Telescope (MEXART) is a full time Interplanetary Scintillation (IPS) array, it is an instrument of the Space Weather National Laboratory in México [www.sciesmex.unam.mx].

A meridional transit radio telescope.

Operation frequency 140 MHz, bandwidth 2 MHz

Location Coeneo Michoacán, México, 20° N, 101° W.

http://www.mexart.unam.mx

http://www.mexart.unam.mx/archivos/data/

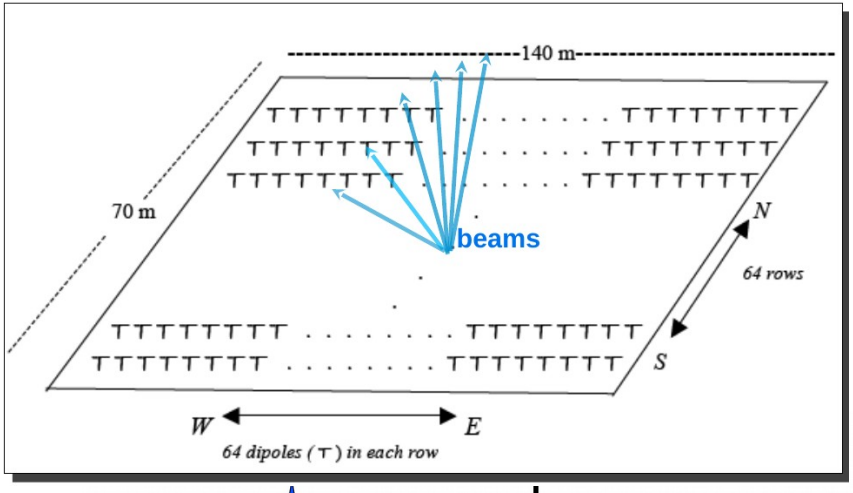

Array of 4096 full wavelength dipoles.
Collecting area = 9800 m²

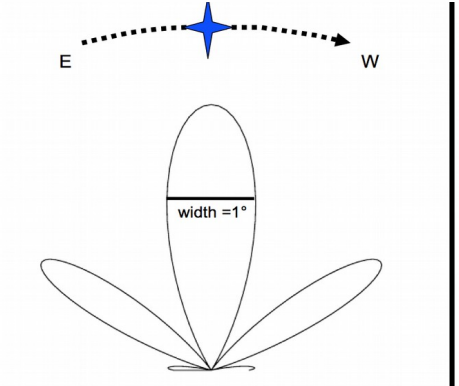

East-west beam pattern and lateral lobes. The beam is fixed at the local zenith.
A source is shown on its east-west trajectory across the beam.

Radio sources record

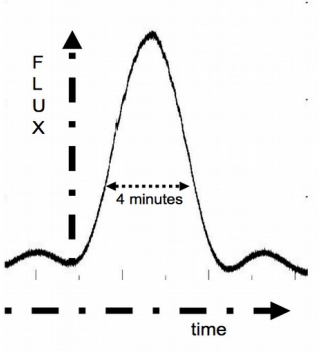

The signal is received from the source, and recorded at a sampling rate of 50/sec (receiver constant = 47 ms).

IPS basic geometry

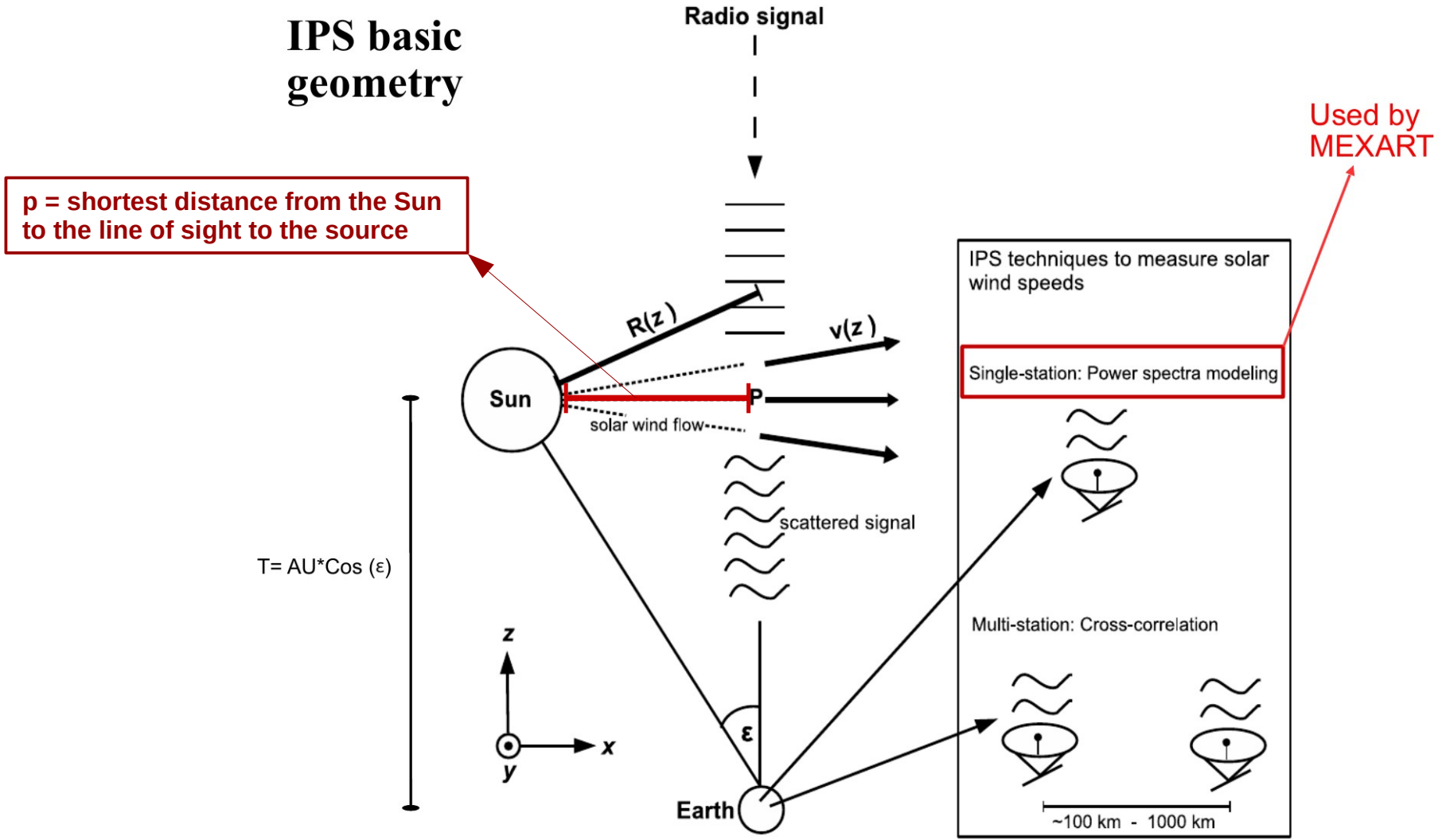

Fourier IPS power spectrum method

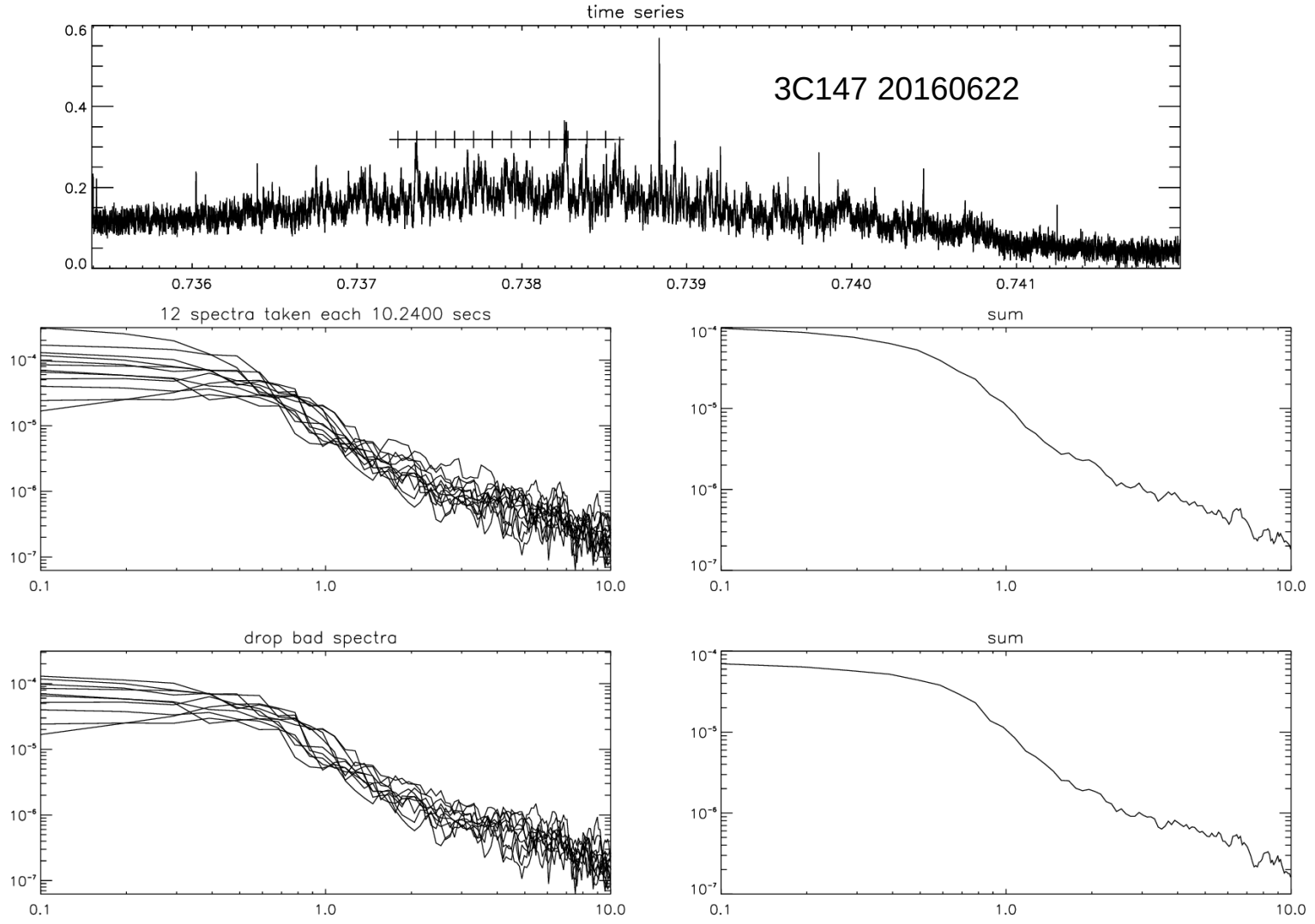

Speed and density of the solar wind by IPS

solar wind speed

$$P(f) = C \int_{z=-T}^{2\mathrm{AU}-T} \mathrm{d}z \frac{1}{V_x(z)} \int_{q_y} \mathrm{d}q_y F_\mathrm{d} F_\mathrm{s} \Phi_{N_\mathrm{e}}$$

$$F_\mathrm{d} = 4\sin^2\left(\frac{q^2 z_0 \lambda}{4\pi}\right)$$ Fresnel $\quad z_0 = z + T$

$$F_\mathrm{s} = \exp\left[-(q z_0 \theta / 2.35)^2\right]$$ Gaussian-visibility

$$\Phi_{N_\mathrm{e}} \propto q^{-\alpha} R^{-\beta}$$ Turbulence density spectrum

Density parameter g for N_e

$$g^2 = \frac{\langle \Delta I^2(r) \rangle}{\overline{\langle \Delta I^2(r) \rangle}}$$

g<1 rarefaction
g>1 density enhancement
g=1 quiet solar wind

$$\langle \Delta I^2 \rangle = \int P(f) \mathrm{d}f$$

Model fitting to power spectra

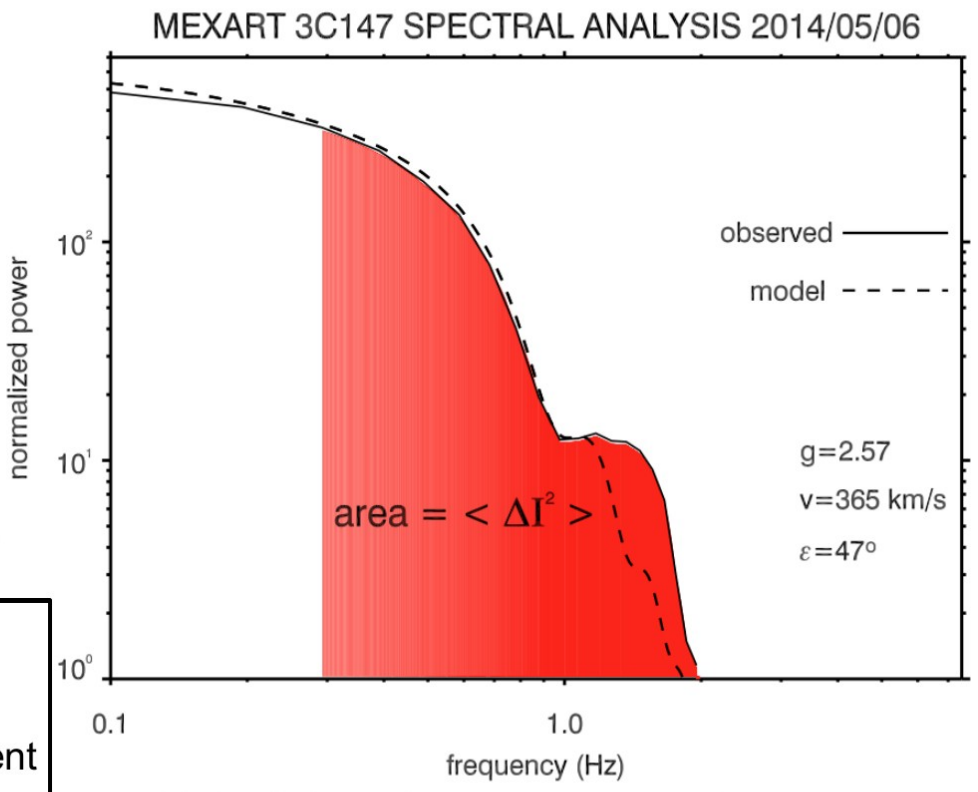

Modeled and observed IPS power spectrum for quasar 3C147

Obtaining the characteristic scale size of the diffraction pattern

Methodology

We apply MFPS to IPS time series to get solar wind speed (v). Below, an example of one observation (3C48 April 4 2018).

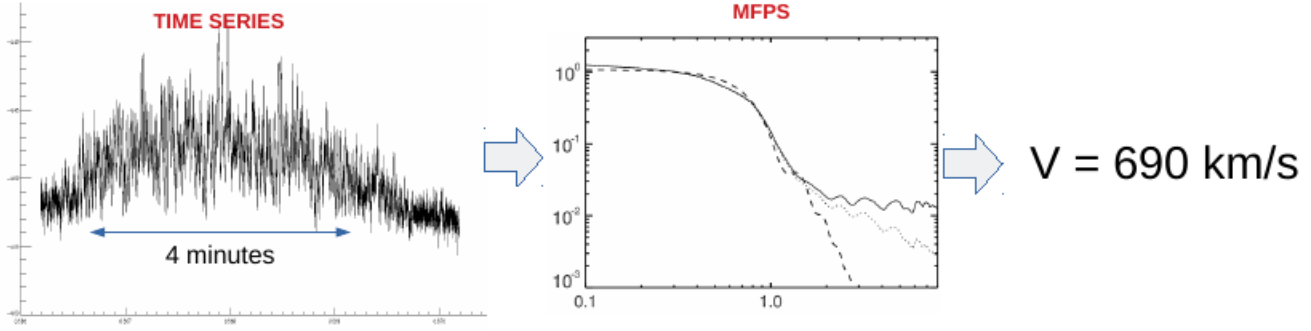

Then, we apply the auto-correlation function to IPS time series and make a Gauss fitting ($\exp\{-x^2/2\sigma^2\}$) to the result. The characteristic temporal frecuency is given by σ, we use σ as the temporal frecuency at which the diffraction pattern moves. Hence, we can estimate the scale of the diffraction pattern by usign $\ell = \sigma * v$, where ℓ is the scale.

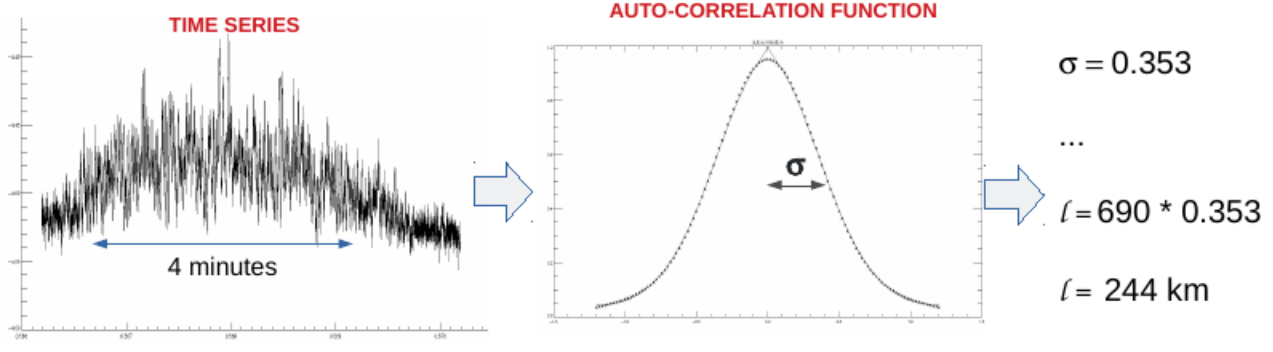

Previous results

We explored the evolution of the scales of the diffraction IPS pattern at diferent elongations (ε). Observations for sources: 3C298 with 17° < ε < 63° (2017) and 3C48 with 29° < ε < 73° (2018) . The scales have a slight decrease in size with the increment of the heliocentric distance p.

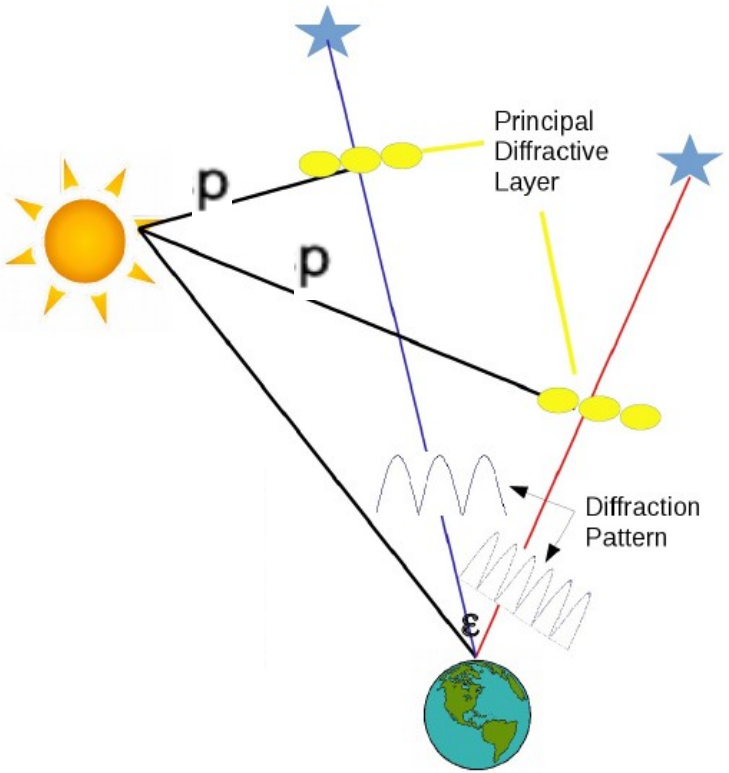

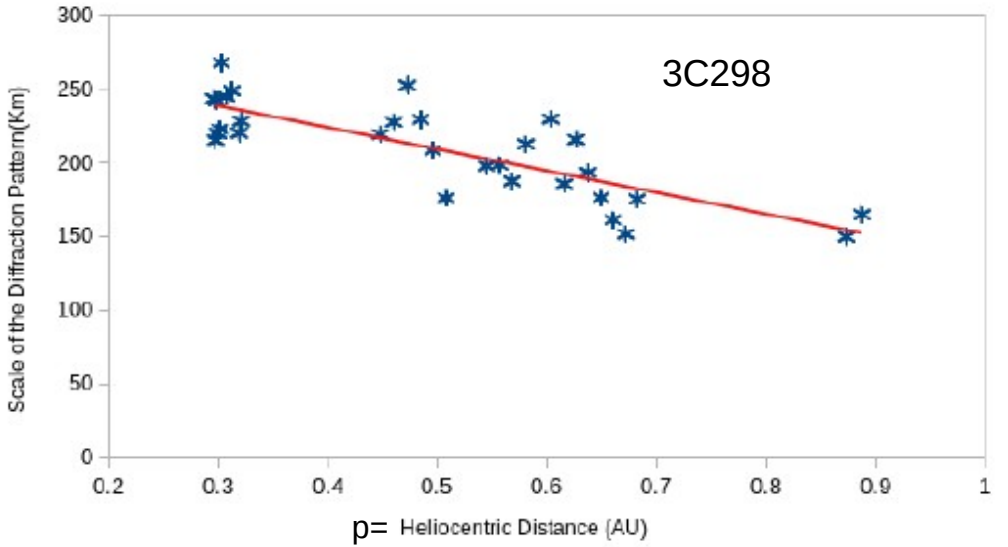

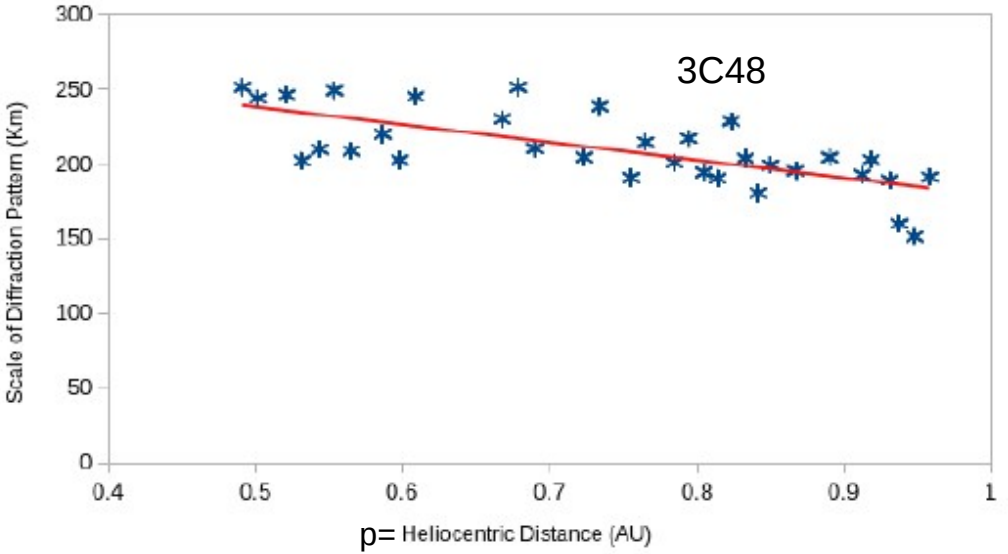

2019 IPS quasar 3C48 observations

From March to July 2019 we recorded 91 observations of 3C48 to follow the evolution of the scales of the IPS radiation pattern and level of scintillation at different heliocentric distances (p).

Here we show the apparent path, as viewed by an observer at Earth, that follows 3C48 in the sky during the epoch of observations, the Sun in red is at the center and blue points indicate the path.

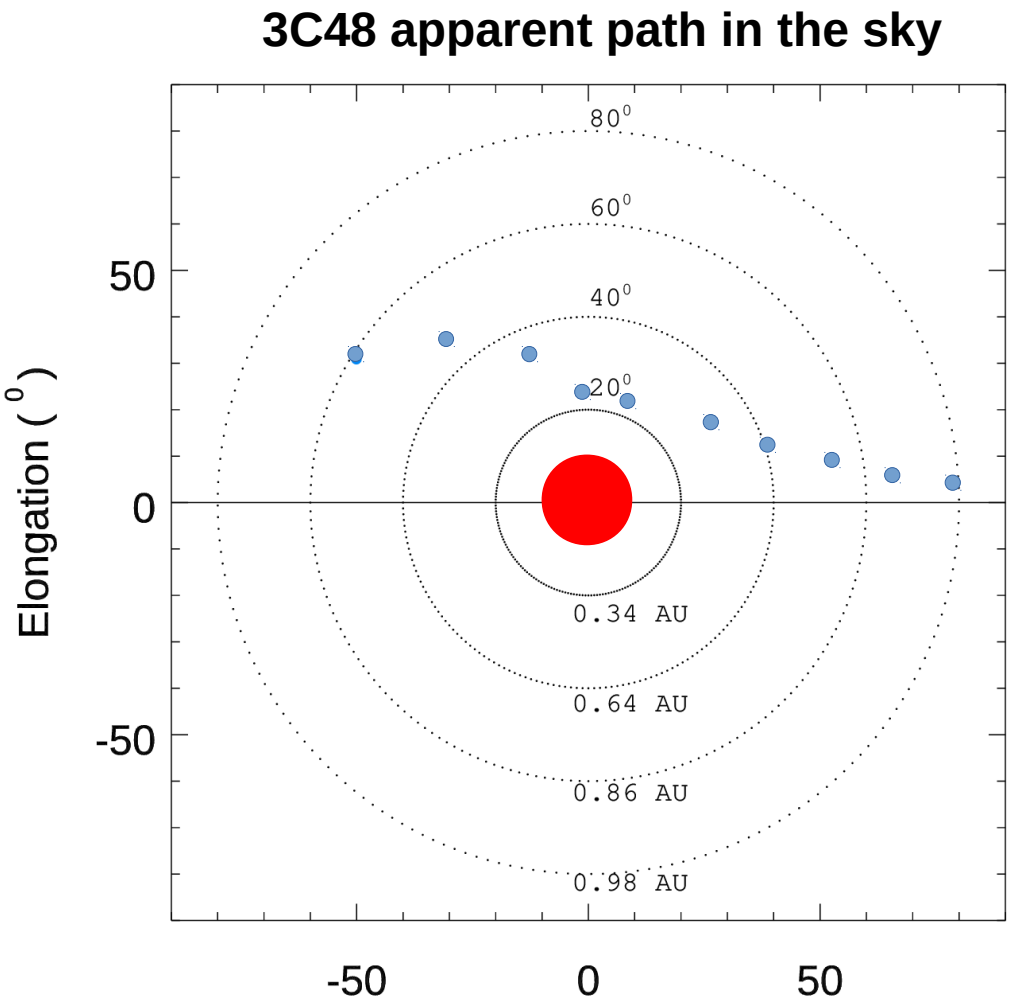

The scales of the IPS diffraction pattern at 140 MHz

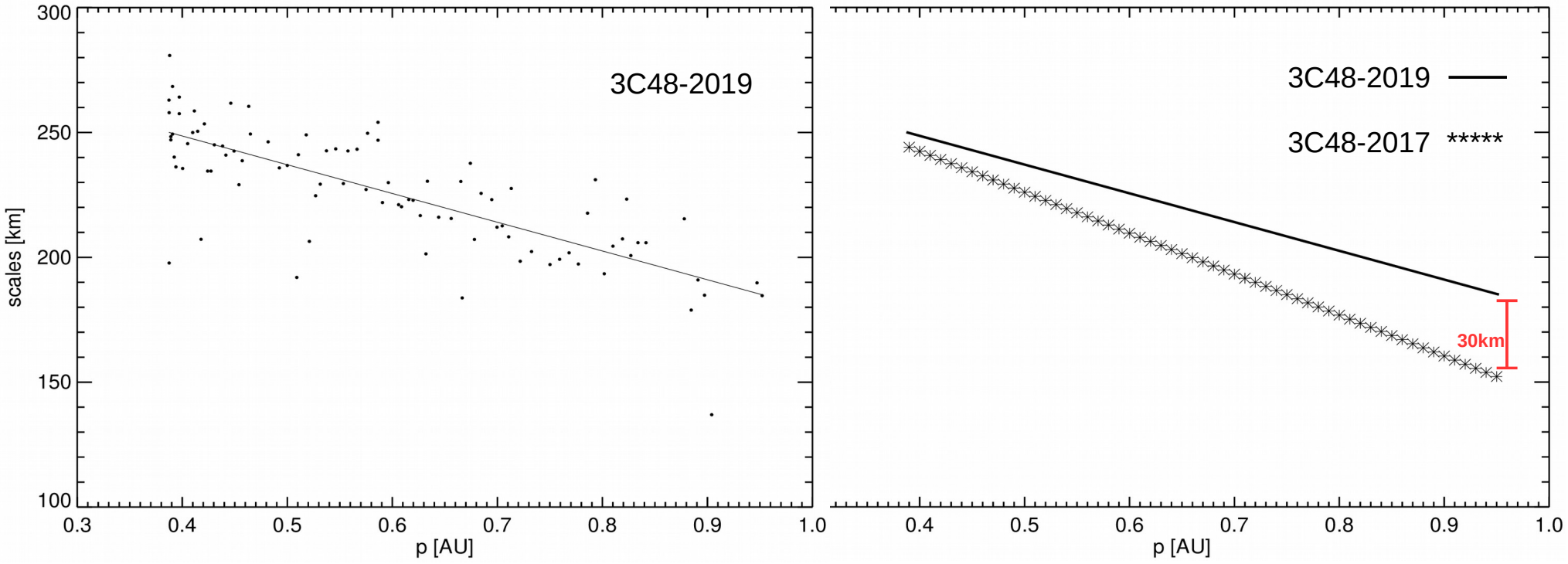

The evolution of the scale of the difraction pattern (140 Mhz) at different heliocentric distances assuming a characteristic scale given by the **σ** of a gaussian shape fitted to the autocorrelation functions

$$e^{-\frac{x^2}{2\sigma^2}}$$

The scales of the IPS diffraction pattern at 140 MHz

By testing the CCF with a sin function we find a correction to the scales

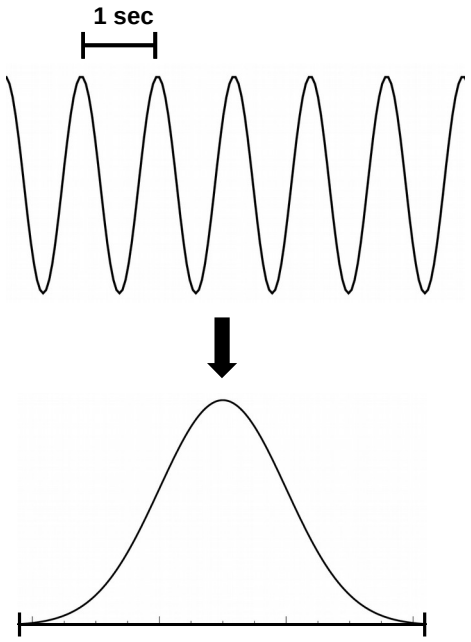

1 sec ≈ 5 σ

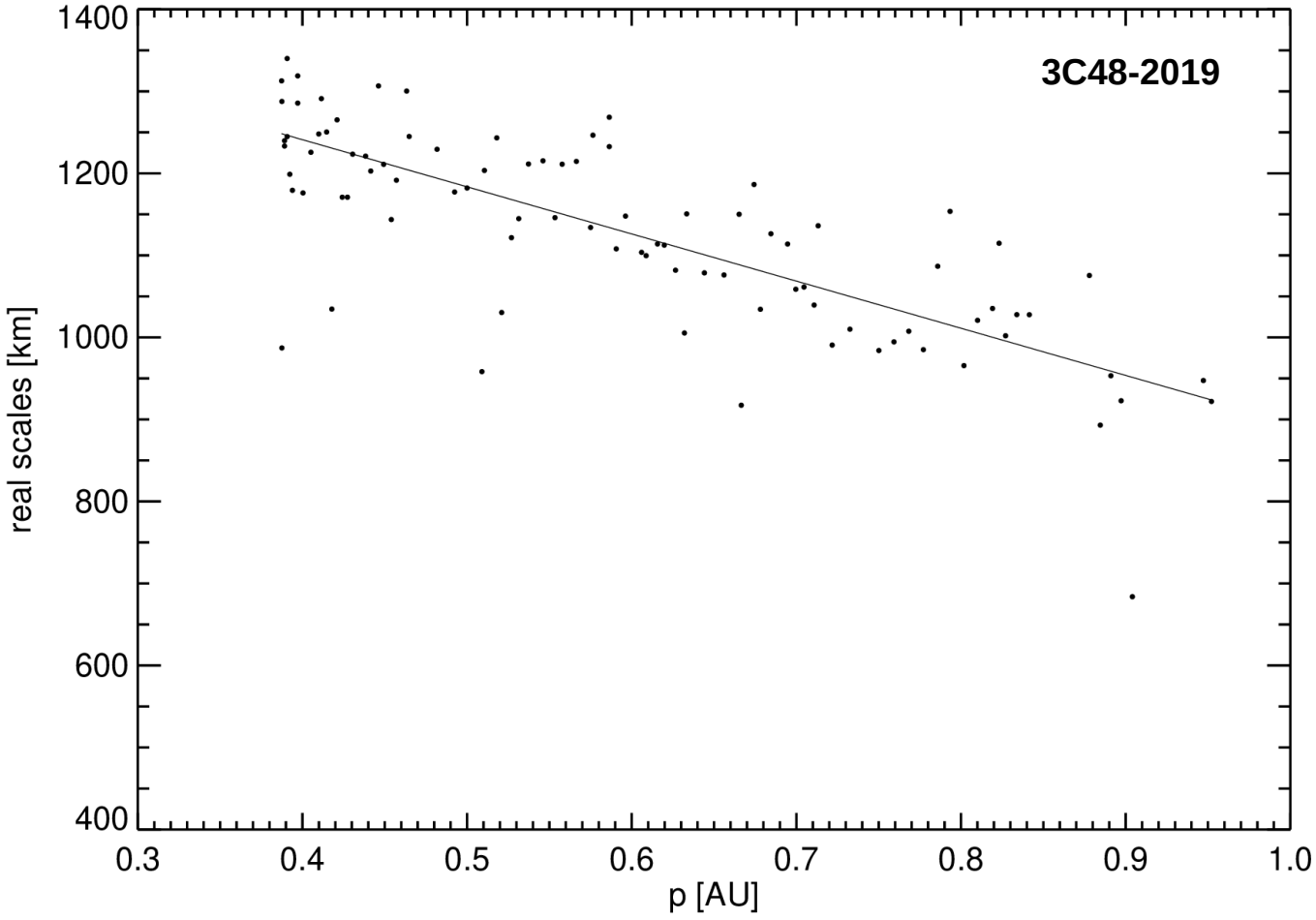

Solar wind speed estimation from ‘calibrated’ period of IPS

The period of scintillation (140 MHz) and solar wind speed are well correlated (-0.7).

A line is fitted to the points which could help to estimate the solar wind speed with a range error.

This way we need only to find the period of a given observation from the Autocorrelation Function (ACF).

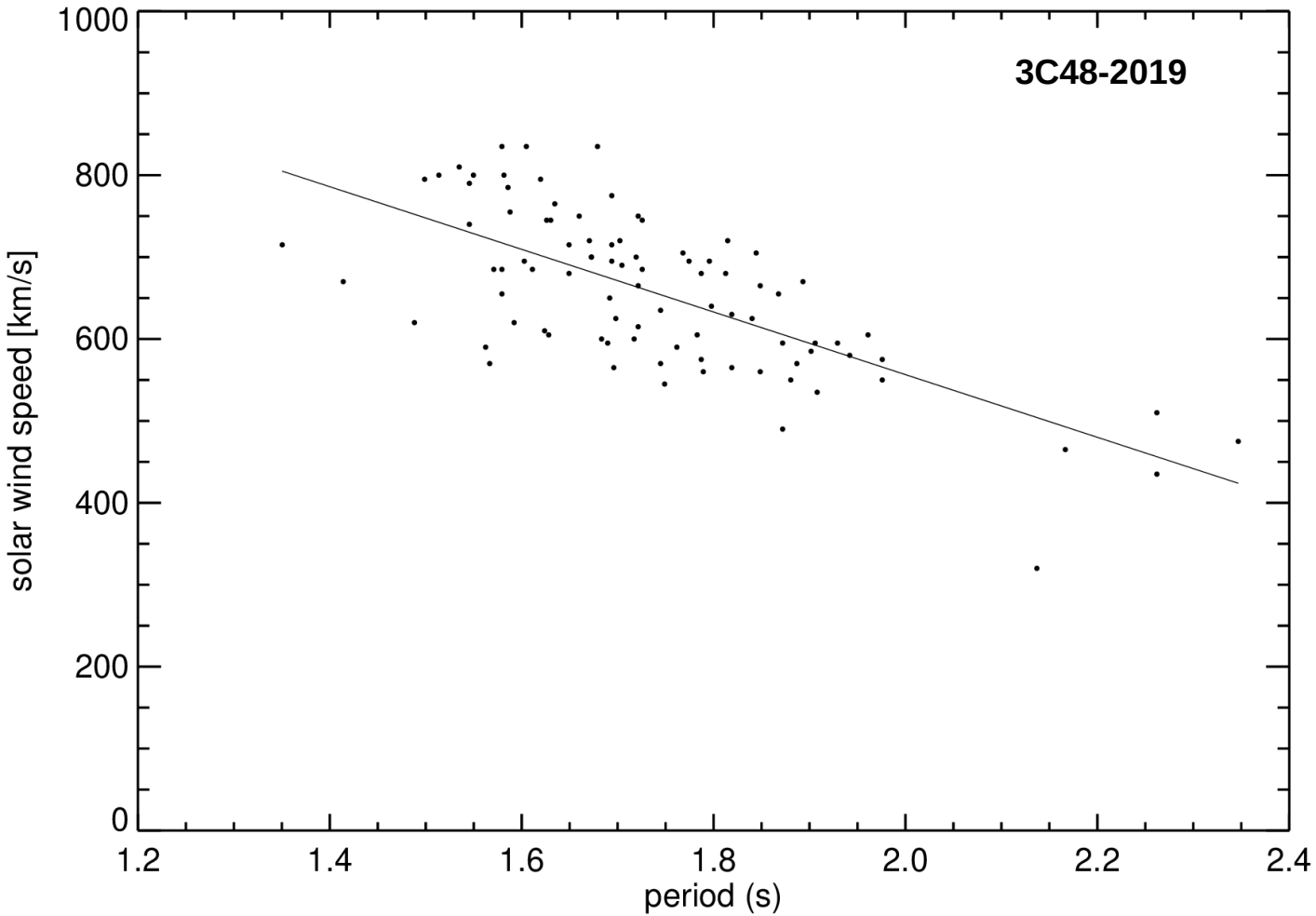

Solar wind speed estimation from ‘calibrated’ period of IPS

High speed CME detection by IPS

Solar wind speeds at three points in the sky from MEXART observations, the point marked with a red oval represents the speed of a CME of 990 km/s, which emerged 2 days earlier.

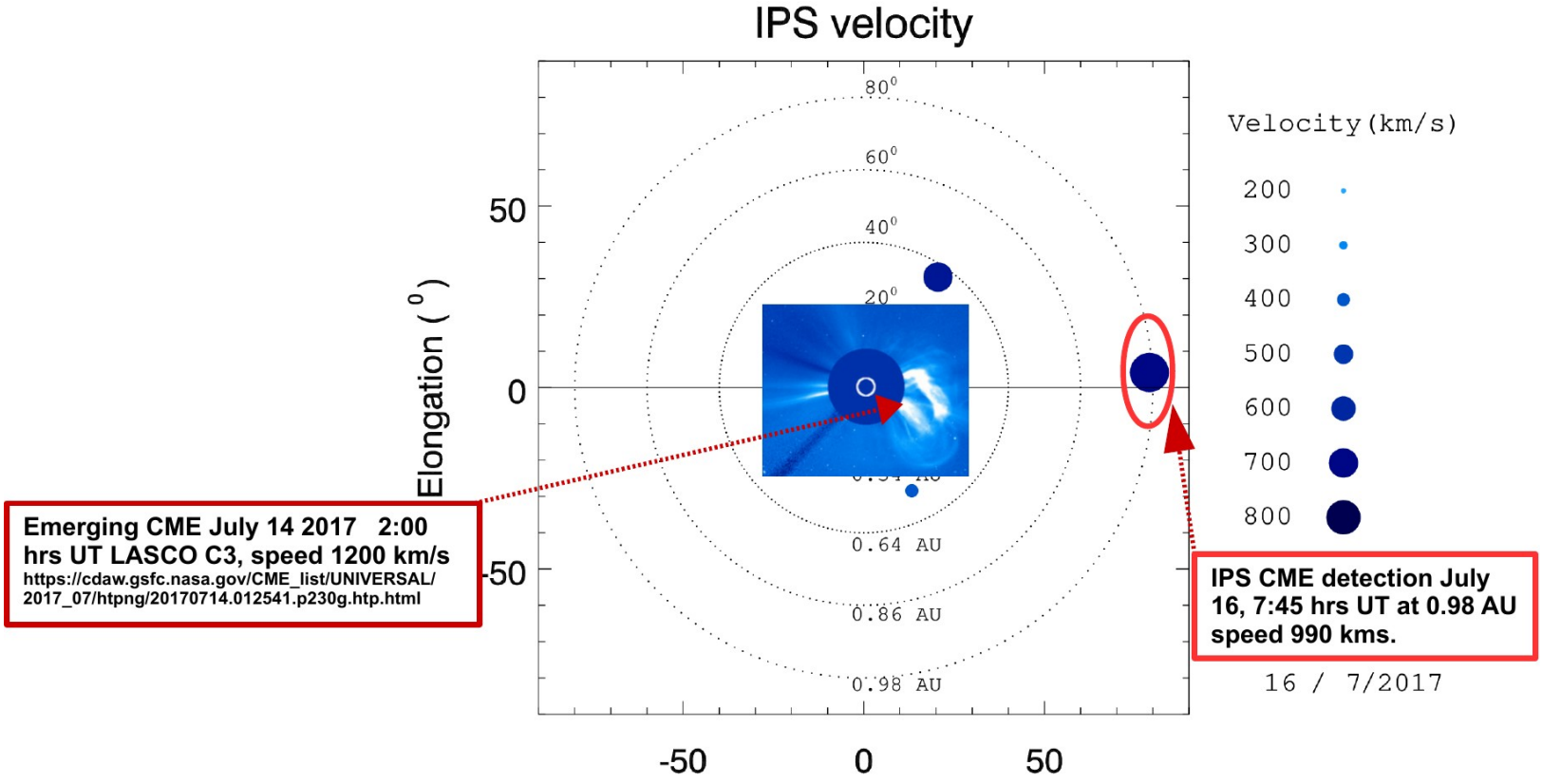

Solar wind speed estimation from ‘calibrated’ period of IPS

Here we test the ‘model’ for the CME speed. We find a short period in the ACF (0.78 sec) of the IPS time-series associated to the 990 km/s CME.

By extrapolating the ‘model’ for the ‘calibrated period-speed’, the CME speed agrees fairly well to the period-speed model.

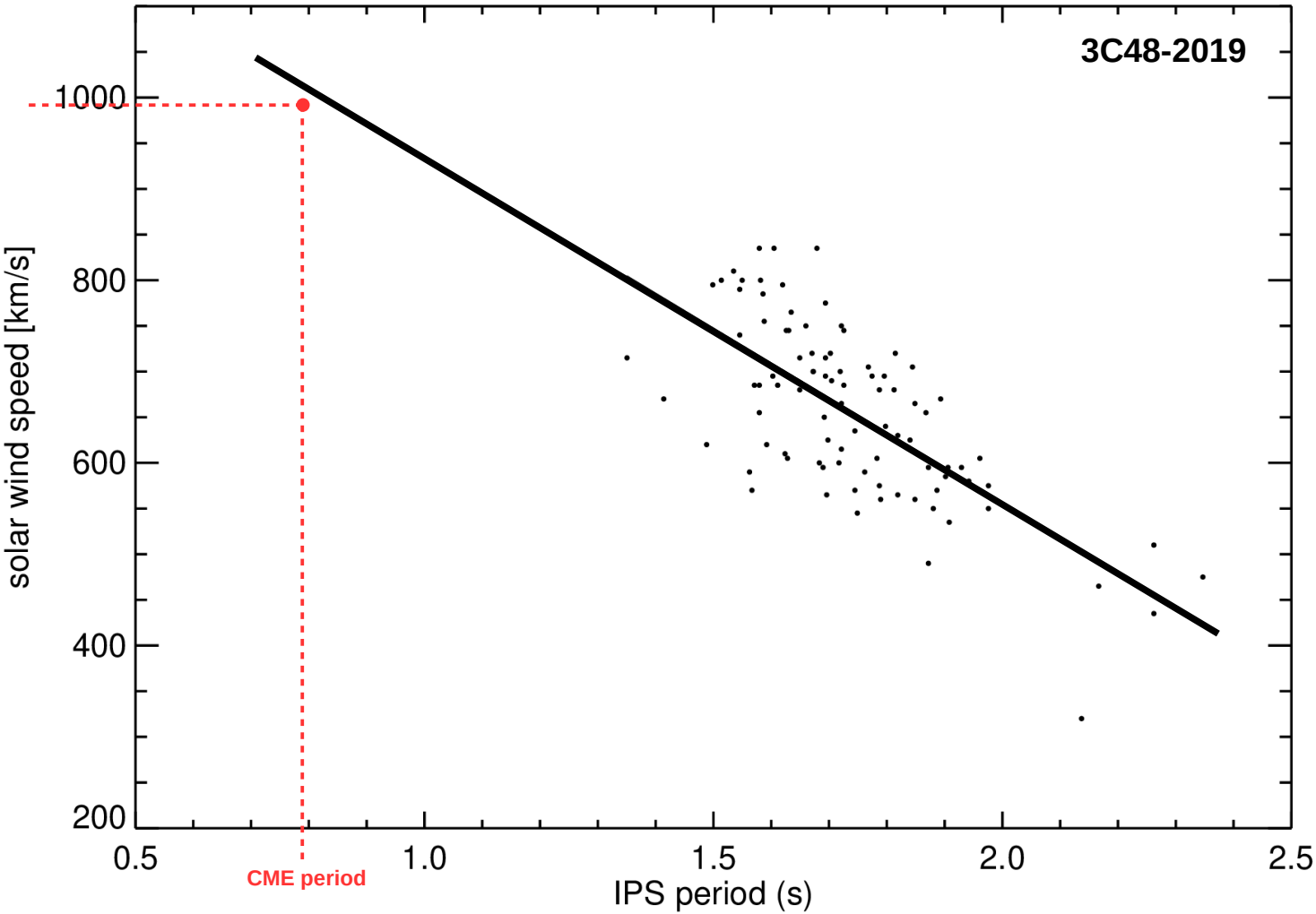

Dependence of electronic density fluctuations Δ*N* on Heliocentric distance using representations of *m*-index

It is known that the average *m*-index in the weak scattering regime can be expresed with

$$m = a\, p^{-b}$$

p = the shortest distance from the Sun to the LOS , b ~ 1.5 – 2.0 and a =constant.

Also, *m* is related to the small-scale density variations (Δ*N*) along the LOS by [Jackson, JGR, 1998]

$$m^2 = \int [\Delta N(z)]^2 W(z)\, \mathrm{d}z$$

where *W(z)* is a weighting factor.

Assuming $\Delta N \propto R^{-\beta}$ and the heliocentric distance to the LOS

$$R^2 = \left[\sin^2\epsilon + (\cos\epsilon - z)^2\right] \mathrm{AU}^2$$

Then the above relations can be combined to obtain:

$$\left[\frac{\sin(\epsilon_1)}{\sin(\epsilon_2)}\right]^{2b} = \frac{\int W(z) / \left[\sin^2(\epsilon_2) + (\cos(\epsilon_2) - z)^2\right]^{\beta} dz}{\int W(z) / \left[\sin^2(\epsilon_1) + (\cos(\epsilon_1) - z)^2\right]^{\beta} dz}$$

For any two different elongations ε1 and ε2 in the weak scattering region

constant *b* don't allow β constant for all the elongations.

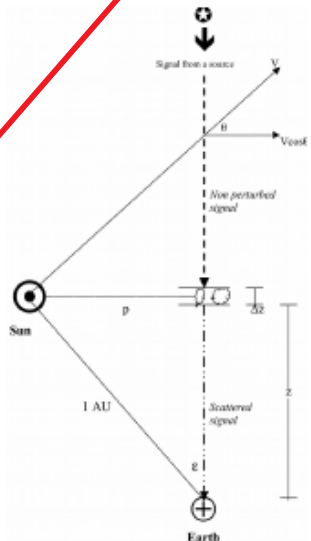

Dependence of m-index and beta parameter

$$\Delta N \propto p^{-\beta}$$

$$m \propto p^{-1.41}$$

b = 1.41

How is related to β ?

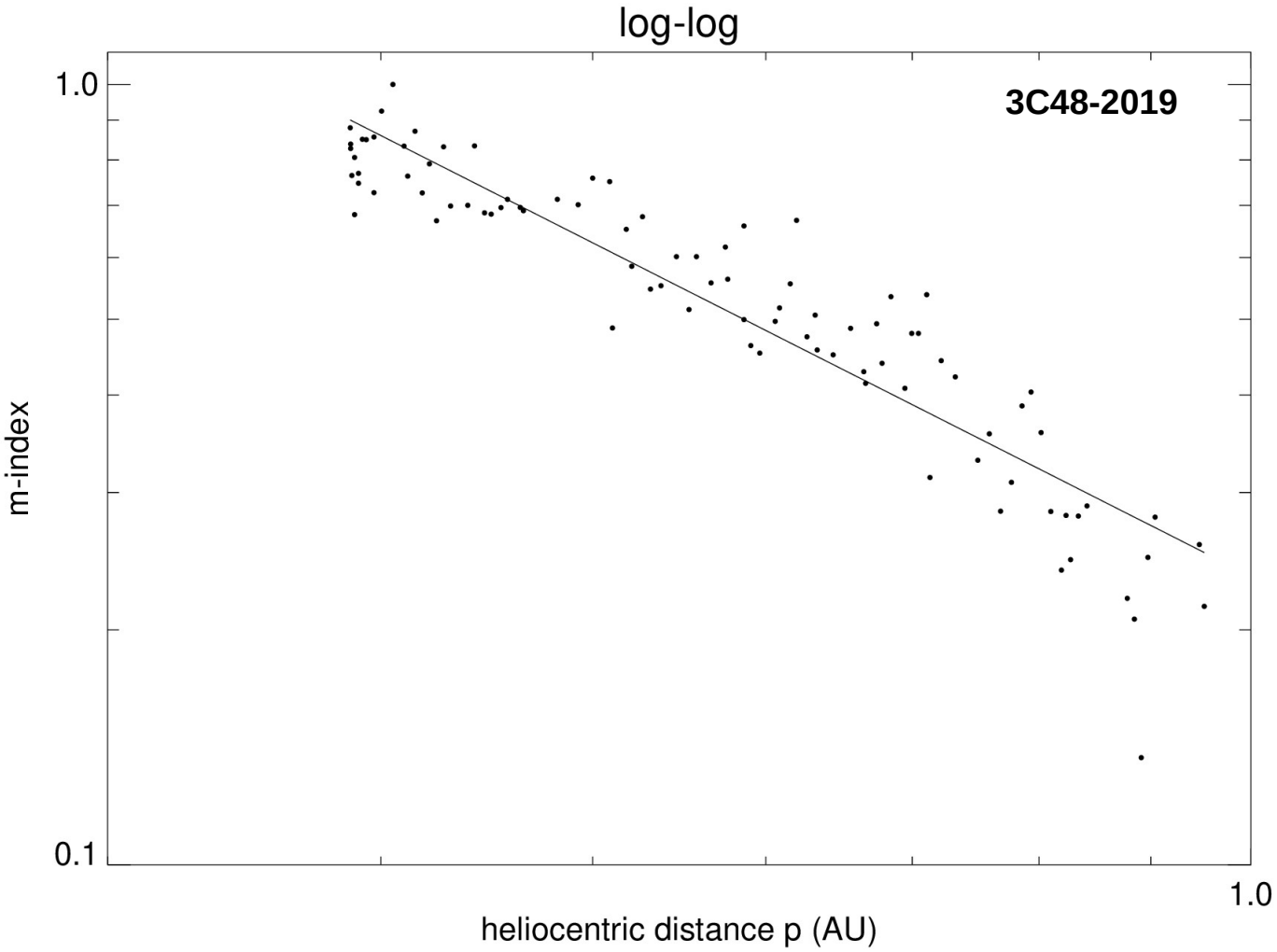

Is the scale of the diffraction pattern *I*(p) related to β?

Beta parameter decrement with heliocentric distance (R) [Mejia-Ambriz, et al. In preparation]

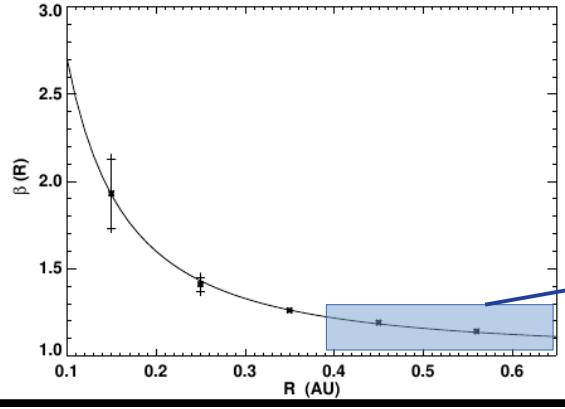

In this interval nearly constant ~ 1.15

Work in progress...

Phase $\phi(x) = r_e \lambda \int \Delta N(x,z) dz$

$\Delta N \propto p^{-\beta}$

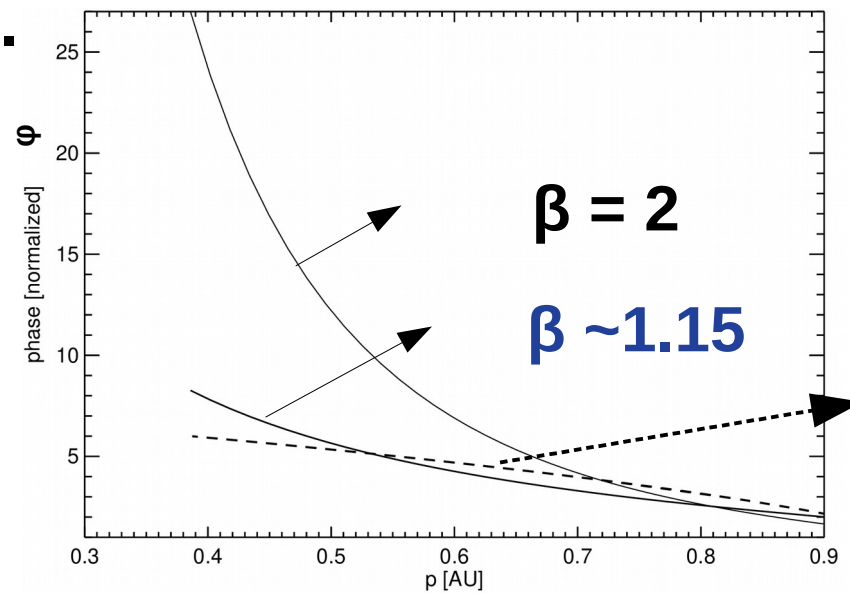

Assuming that phase is also described by the sales of diffraction pattern (*I*) and increases with the distance of the principal diffractive layer

$$\phi \approx (2\pi x/l)\cos(\epsilon)$$

$$\cos(\epsilon) = \sqrt{1 - p^2}$$

CONCLUSIONS

The scales of the diffraction pattern seems to be higher than the small-scale density fluctuations observed at meter wavelengths. These small-scales are considered to be ~200-300 km.

The ‘calibrated’ of speed – perido/frequency could privide an estimation of solar wind speed for a given observed period/ips frequency without using the MFPS. A range error should be estimated.

Supposing $\Delta N \propto p^{-\beta}$ **, we find β(p) < 2 from 0.4 to 1 AU.**

We suppose isotropic solar wind, in further studies using different sources could provide an insight about the evolution of the diffraction scales according to apparent paths of the sources in the sky.

LANCE

Laboratorio Nacional
de Clima Espacial

IGUM

INSTITUTO de GEOFÍSICA
Unidad Michoacán

OBSERVATORIO DE CENTELLEO INTERPLANETARIO - COENEO MICHOACÁN

MEXART

The wavelet technique applied to interplanetary and ionospheric scintillation

Julio Mejia-Ambriz[1], E. Romero-Hernandez (2), M.A. Sergeeva (1), E. Aguilar-Rodriguez (3), J.A. Gonzalez-Esparza (3), M. Rodriguez-Martinez (4), V. De la Luz[2] , J.A. Gonzalez-Esparza[2] , P. Villanueva-Hernandez[2], E. Andrade-Mascote[2] , A. Espinosa-Jimenez[2] , J.L. Godoy [2]

[1]CONACyT, Laboratorio Nacional de Clima Espacial (LANCE), Instituto de Geofísica, UNAM
[2] LANCE, Instituto de Geofísica, UNAM

Scintillating Science: Cutting-Edge Science Achieved Through the Observations of Radio Scintillation

July 2019

The wavelet Transform

The Wavelet Transform (WL) is a tool for analyzing localized variations of power within a non-stationary time series by decomposing it into time–frequency space.

For a time series $\{x_n\}$ with δt separation

$$W_n(s) = \sum_{n'=0}^{N-1} x_{n'} \psi^* \left[\frac{(n'-n)\delta t}{s} \right]$$

n represents time, s scale or frequency (1/s) and Ψ must satisfy different conditions to be a considered a WL transform.

Here we use the Morlet representation with 2dt resolution given by

$$\psi_0(\eta) = \pi^{-1/4} e^{i\omega_0 \eta} e^{-\eta^2/2}$$

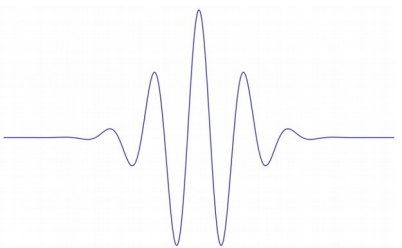

Program routines for IPS used in this work were adapted from Torrence and Compo [1998]. De Moortel et. al, 2014 show why Morlet function is better for IPS.

Data treatment

To obtain an accurate estimate of the physical parameters of the small scale density fluctuations in the solar wind or ionosphere via WT to scintillation, two things are required:

1) an appropriate treatment of the time series.
a) high signal-to-noise ratio (S/N) of the intensity fluctuations.

Appropriate treatment here:

Detrending (S. Mushini 2016 detrending via WT), filtering, and smoothing the data such that the resulting power spectra emphasize the characteristics from IPS and minimize the influence of external noise.

Materassi and Mitchell 2007

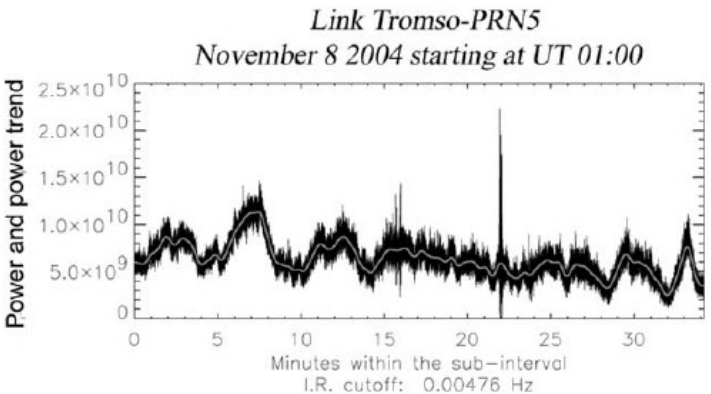

GPS receiver

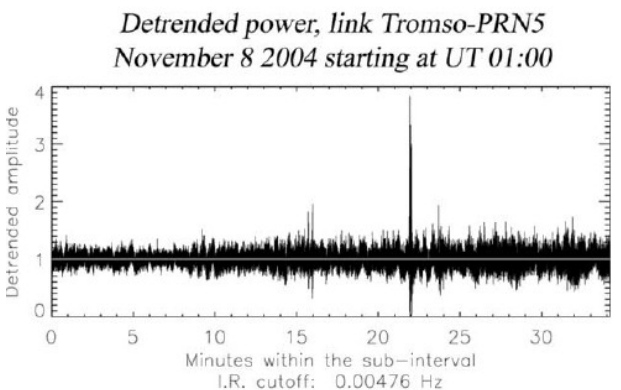

detrending

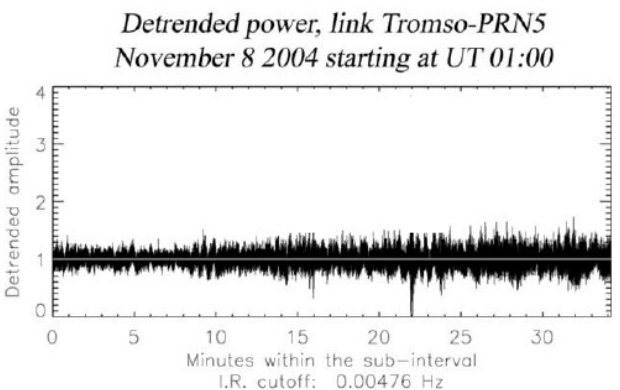

filtering

Wavelet technique in IPS

First IPS WL analyses were reported [Aguilar-Rodriguez, et al. 2014] with observations at 327 MHz by the Solar Wind Imaging Facility Telescope in Toyokawa, Japan. The aim was to study the evolution of index of scintillaion for this source during 2012.

Above in figure a transit of 3C48 where low-frequency trend is removed with a high-pas filter to reduce the data contamination due to possible ionospheric scintillation. Below the Wavelet Transform (WT) applied to the subtracted time series.

The dashed lines indicate the frequency range where IPS is commonly observed (i.e., from 0.3 Hz up to 2 Hz). The power is plotted in logarithm.

Time resolution = 2Δt= 40ms

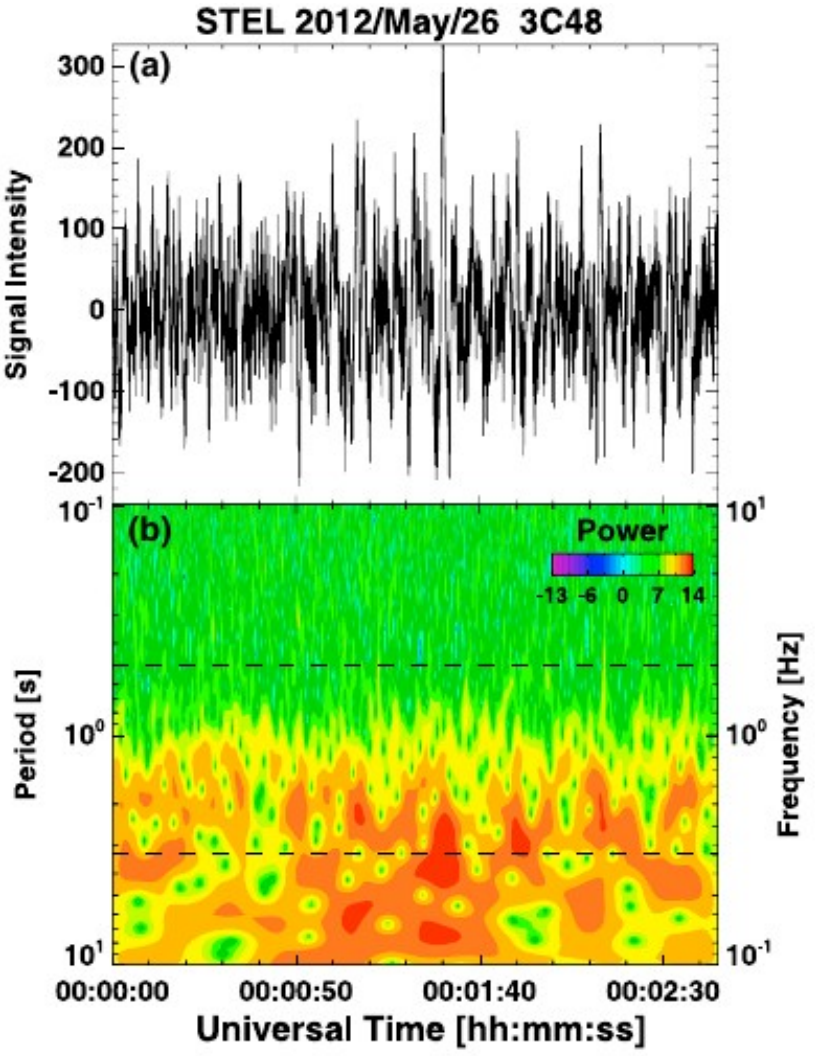

Proposed wavelet index for IPS

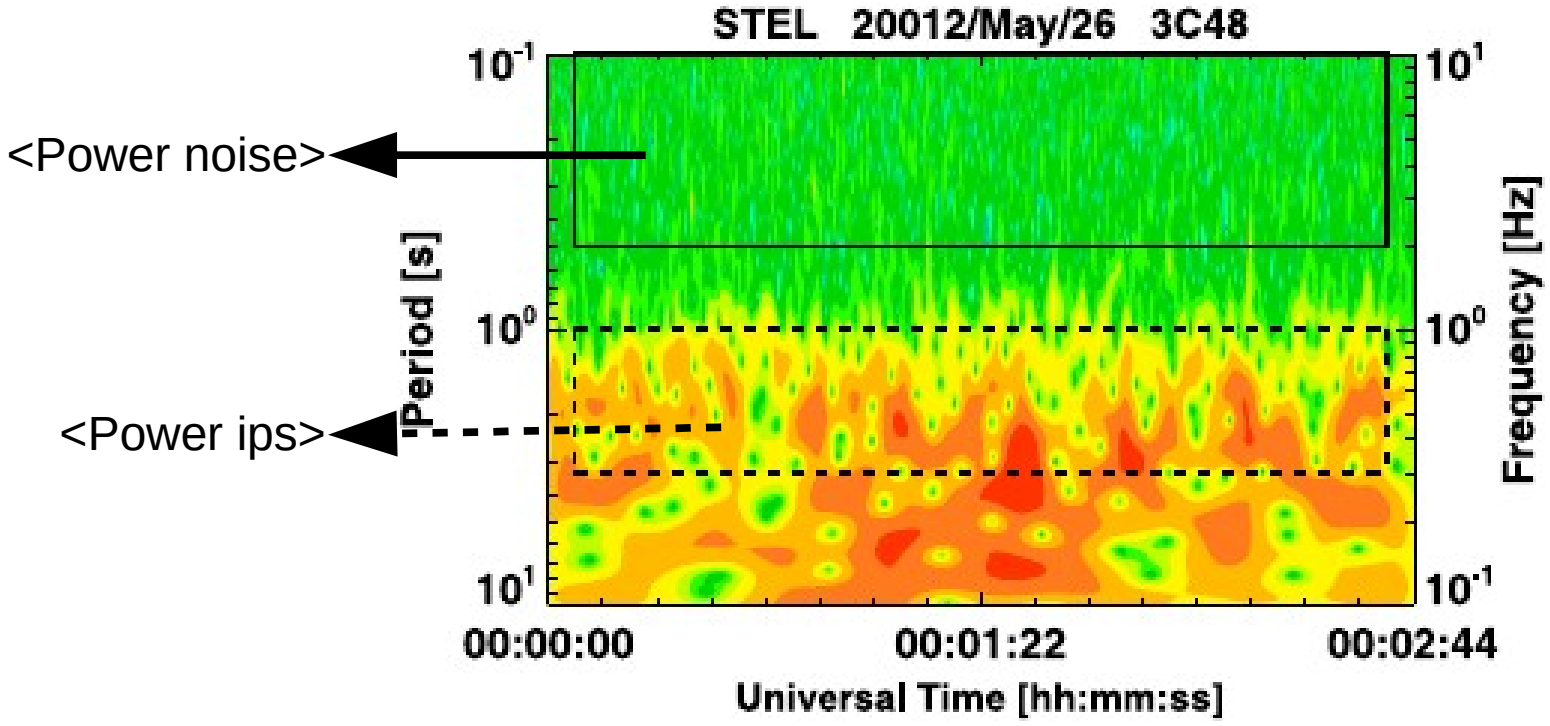

Index = <Power ips> - <Power noise>

In the case of Ionospheric Scintillation this method could be tested to obtain S_4

IPS sintillation index

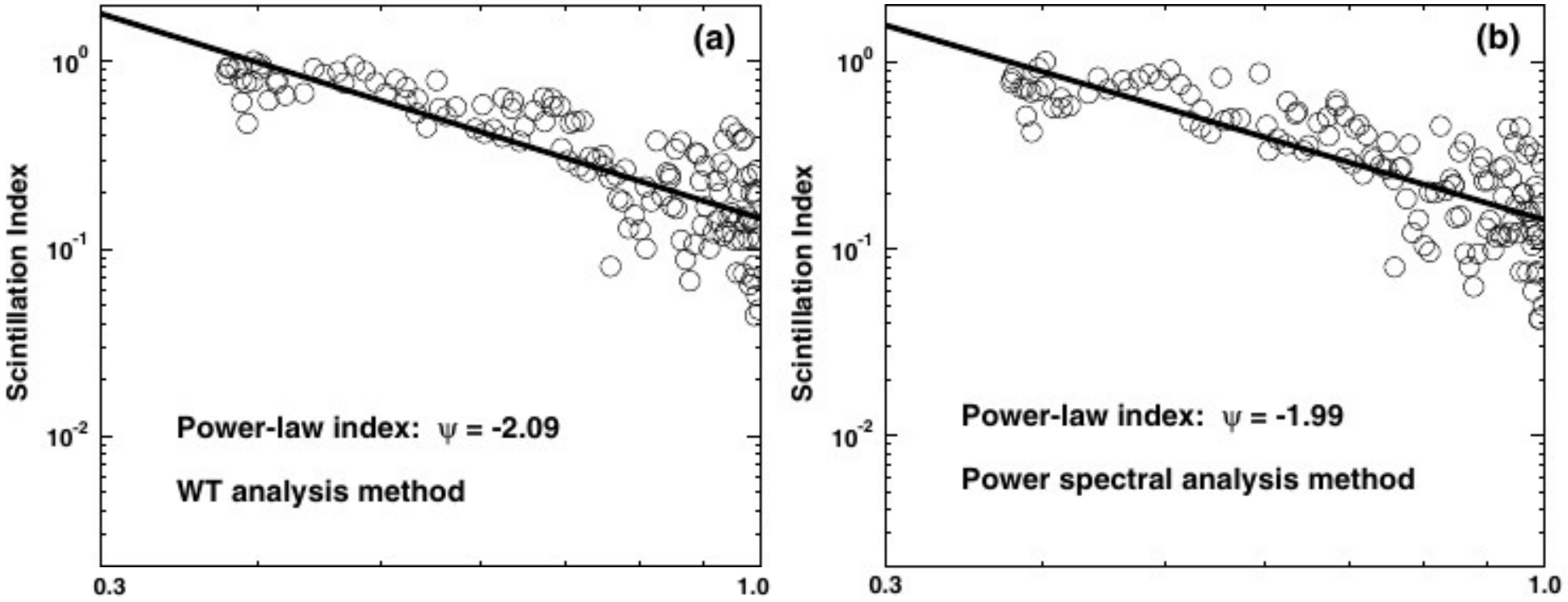

With the WT analysis measuring indeces at different heliocentric distances, p, we find that the index deacays as a power law function p^-2.09.

With the power spectral analysis (area under the power spectrum) we find p^-1.99.

Thus the alternative WT method can be used to measure m^2 indexes and should works for IONS.

Removing bad data

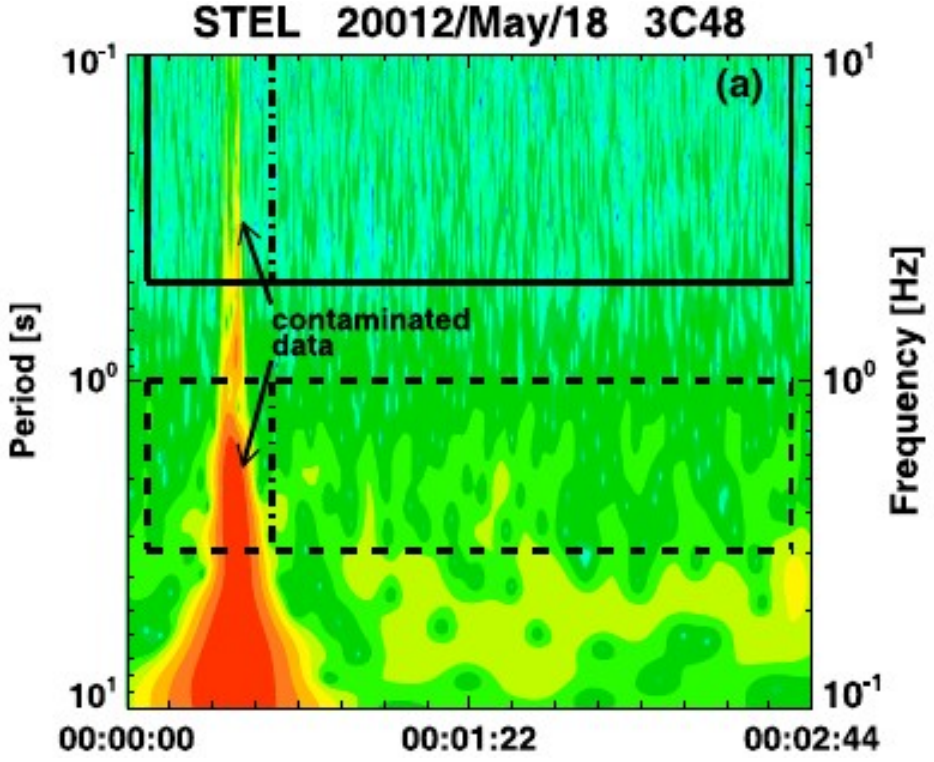

The vertical dash-dotted line that shows the beginning of the time interval selected (i.e., from the dash-dotted line to the right) to skip contaminated data. This method is more flexible to than Fourier analyses.

CONE OF INFLUENCE

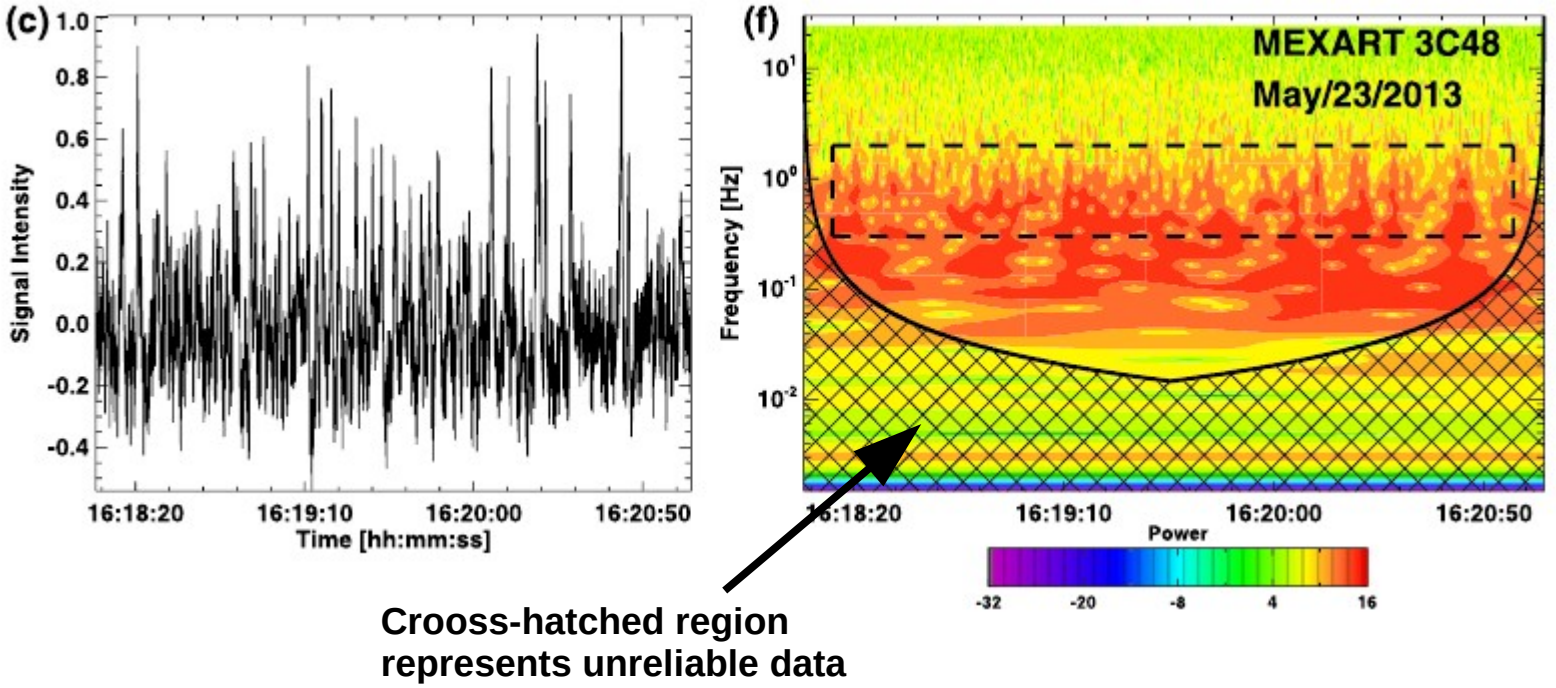

Crooss-hatched region represents unreliable data

Discontinuity edge effect produces a cone of influence. The WT that are inside the area formed by the time axis and the cone are subject to these edge effects and are considered unreliable. The window of the IPS spectral frequency is clearly seen outside the cross-hatched regions that represent the COI.

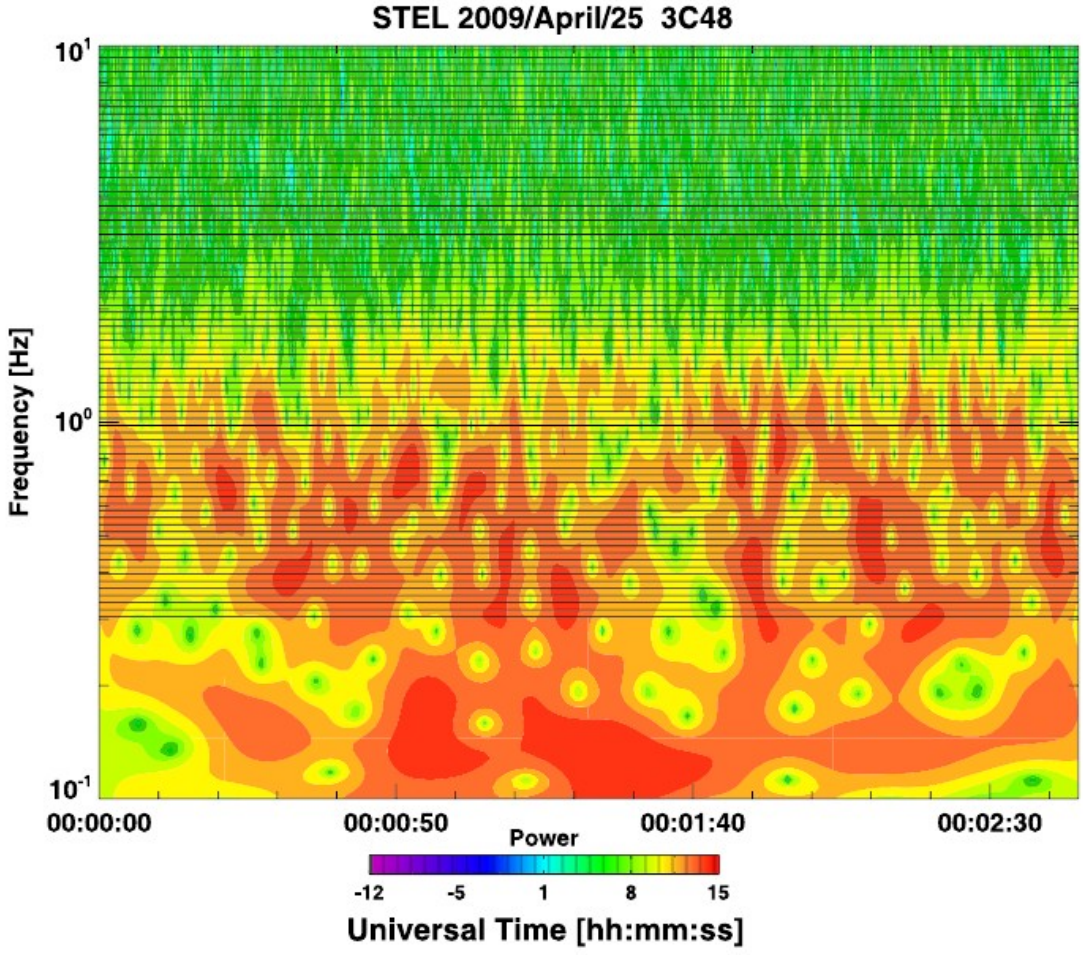

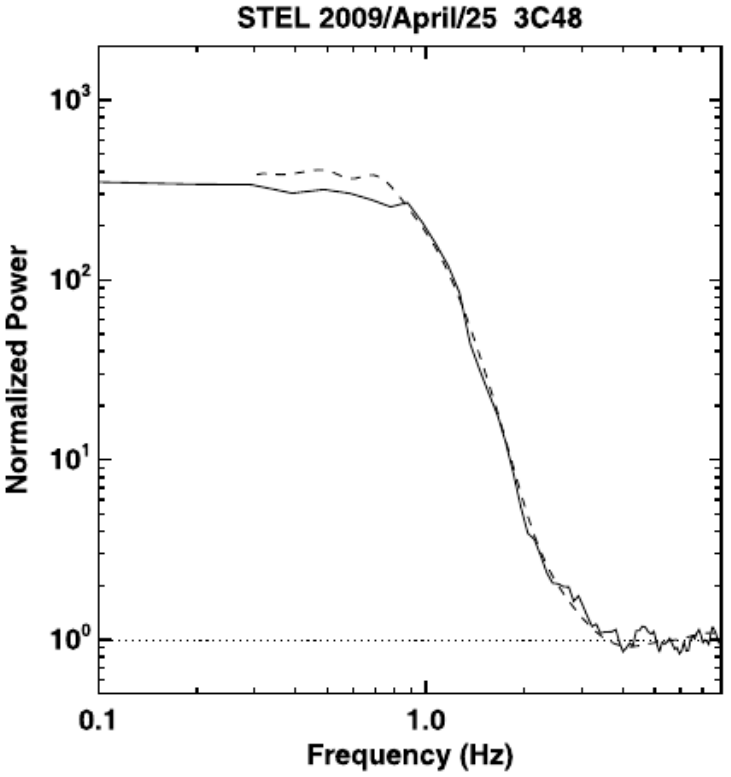

From frequency channels we can obtain the IPS power spectra. The dashed line represents the spectrum obtained with the WT The solid line shows the spectrum with the Fourier transform. Power spectra from WL are slightly cleaner with an apparent level of intensity fluctuations that is enhanced (≈ 13 % higher).

Solar wind speeds calculated with power spectra

Solar wind speeds

Scintillation level

$$\langle \Delta I^2 \rangle = \int P(f)\mathrm{d}f$$

Date	WT speed [km s^{-1}]	FFT speed [km s^{-1}]	WT $\langle \Delta I^2 \rangle$	Fourier $\langle \Delta I^2 \rangle$
21 April 2009	625 ± 100	630 ± 95	245	198
23 April 2009	660 ± 57	655 ± 62	235	223
24 April 2009	640 ± 75	655 ± 45	286	254
25 April 2009	655 ± 52	670 ± 32	288	253
28 April 2009	615 ± 122	625 ± 115	186	156
8 May 2012	380 ± 85	380 ± 55	302	247
9 May 2012	420 ± 102	430 ± 57	182	209
29 March 2013	395 ± 67	395 ± 57	74	62
8 April 2013	335 ± 60	340 ± 60	150	134
26 April 2013	450 ± 95	450 ± 65	145	132
27 April 2013	430 ± 77	415 ± 77	291	250
28 April 2013	380 ± 65	390 ± 50	440	374

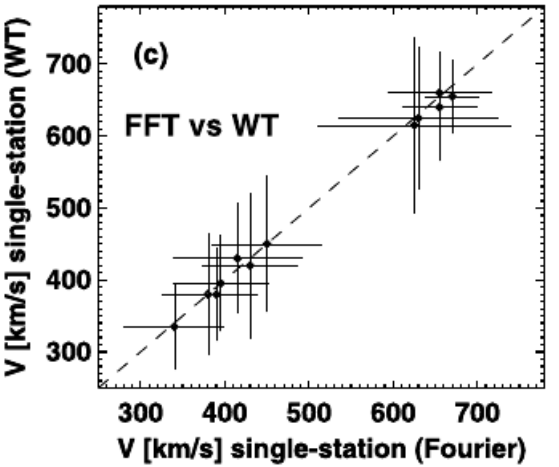

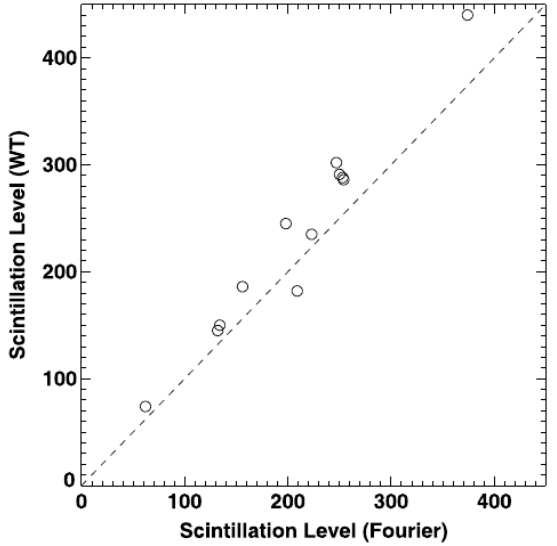

Wavelet transform to ionospheric scintillation records at 140 MHz 20°N

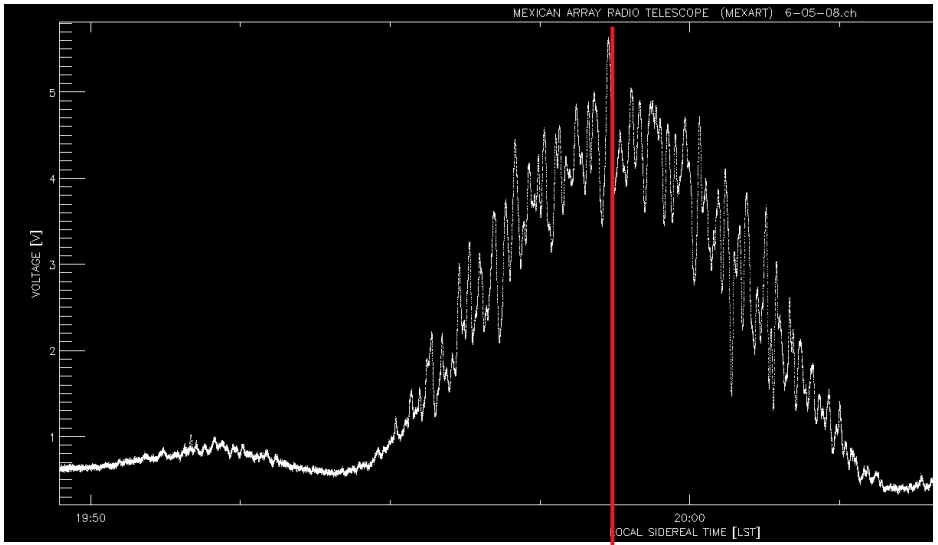

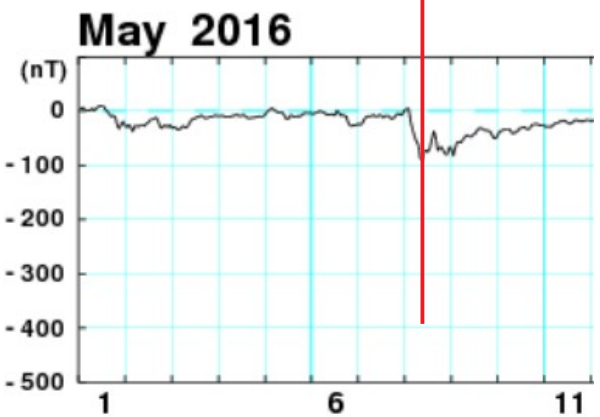

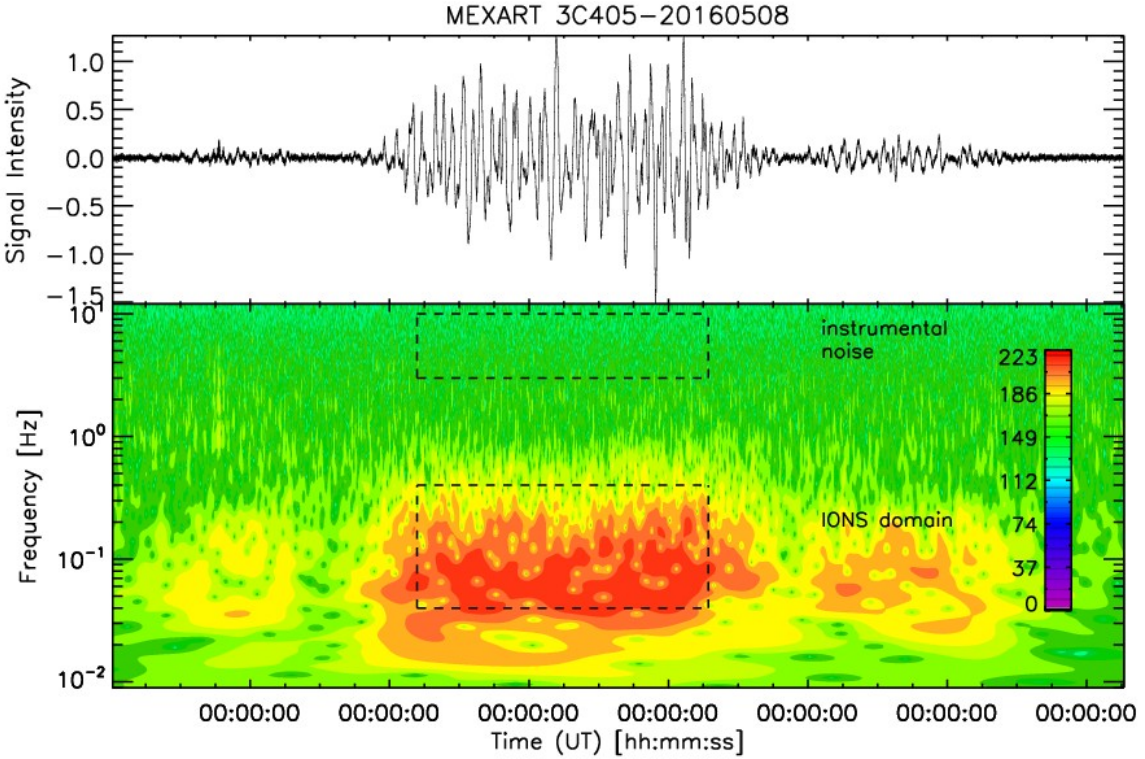

Cygnus A (3C405) observation during a strong geomagnetic storm. Exhibits high level of scintillation.

Wavelet transform to ionospheric scintillation records at 140 MHz 20°N

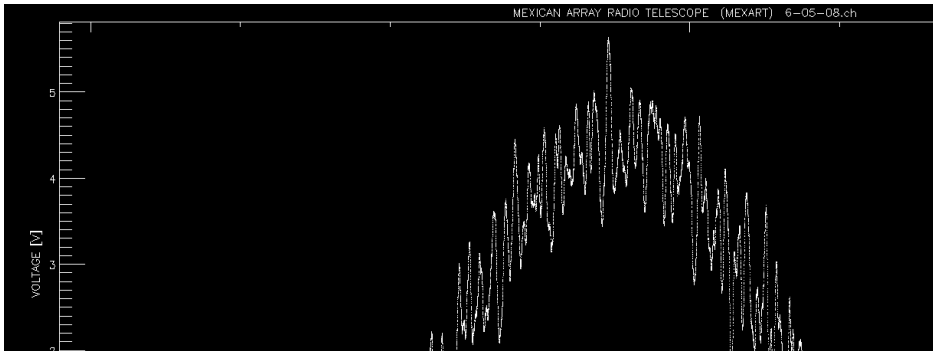

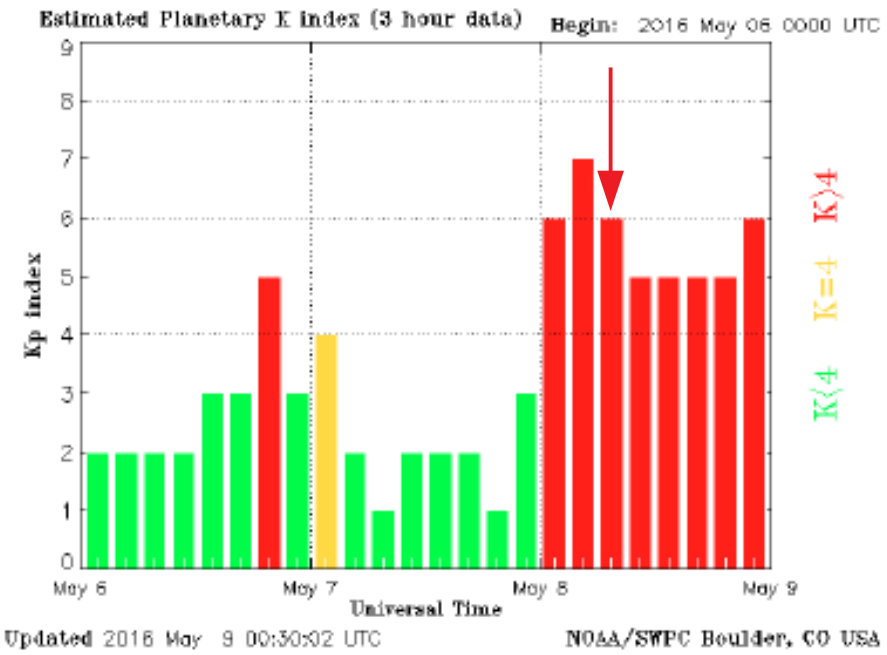

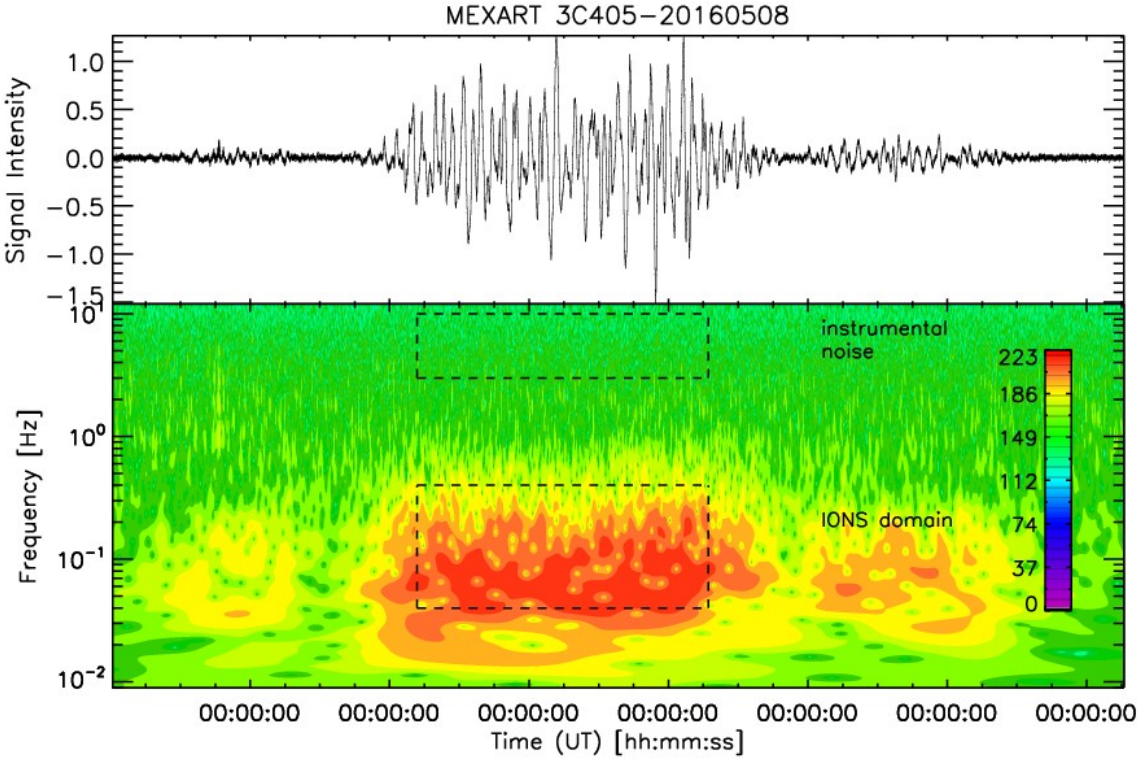

Space weather studies using WT in IONS

By using IONS observations of MEXART-140MHz [Rormero Hernández, et al 2107], we explore the relation of level of scintillation with the ionospheric ionospheric disturbances over Mexico associated to solar transient

Radio source	R.A.	Declination	Flux at 140 MHz [Jy]	Observational interval
3C144	05:34:30	22°01′00″	1660	Jan 2014–Dec 2015
3C274	12:30:49	12°23′28″	924	Jan–Sept 2014, Jan–June 2015
3C405	19:59:28	40°15′37″	8985	Jan 2014–Dec 2015
3C461	23:23:28	58°48′42″	13,551	Jan 2014–Dec 2015

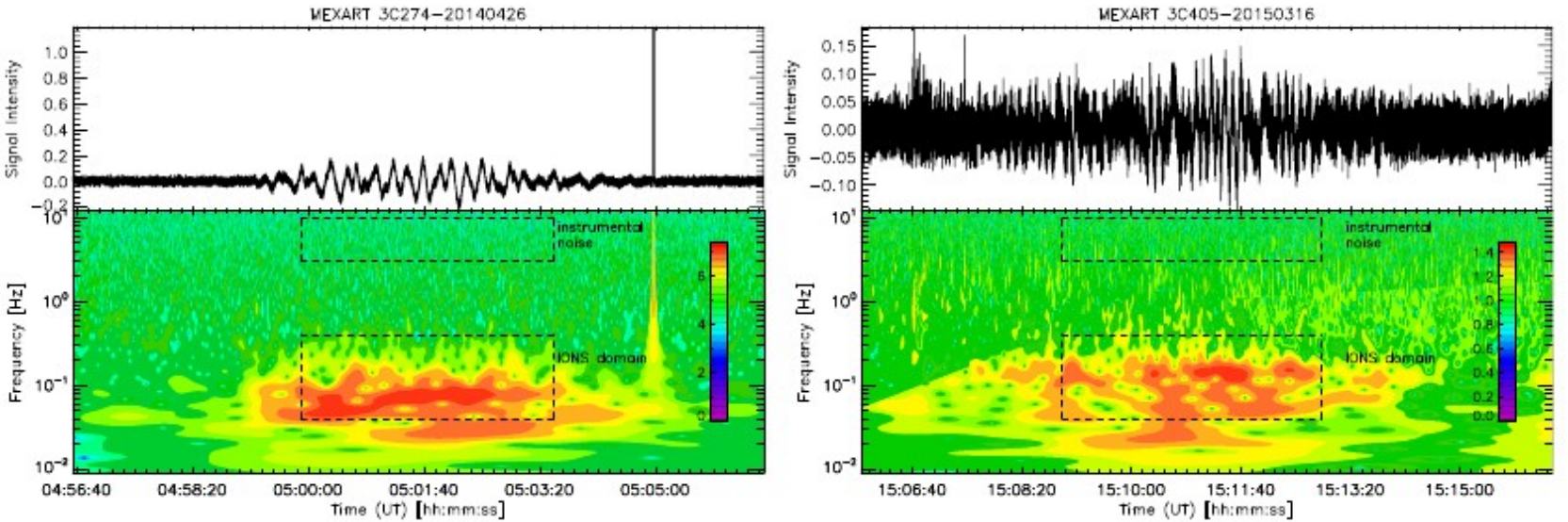

To obtain a ionospheric scintillation index (S_4), the instrumental noise is subtracted from the total power of the IONS domain. The scintillation intensity corresponds to the square root of the total power of the IONS range without instrumental noise.

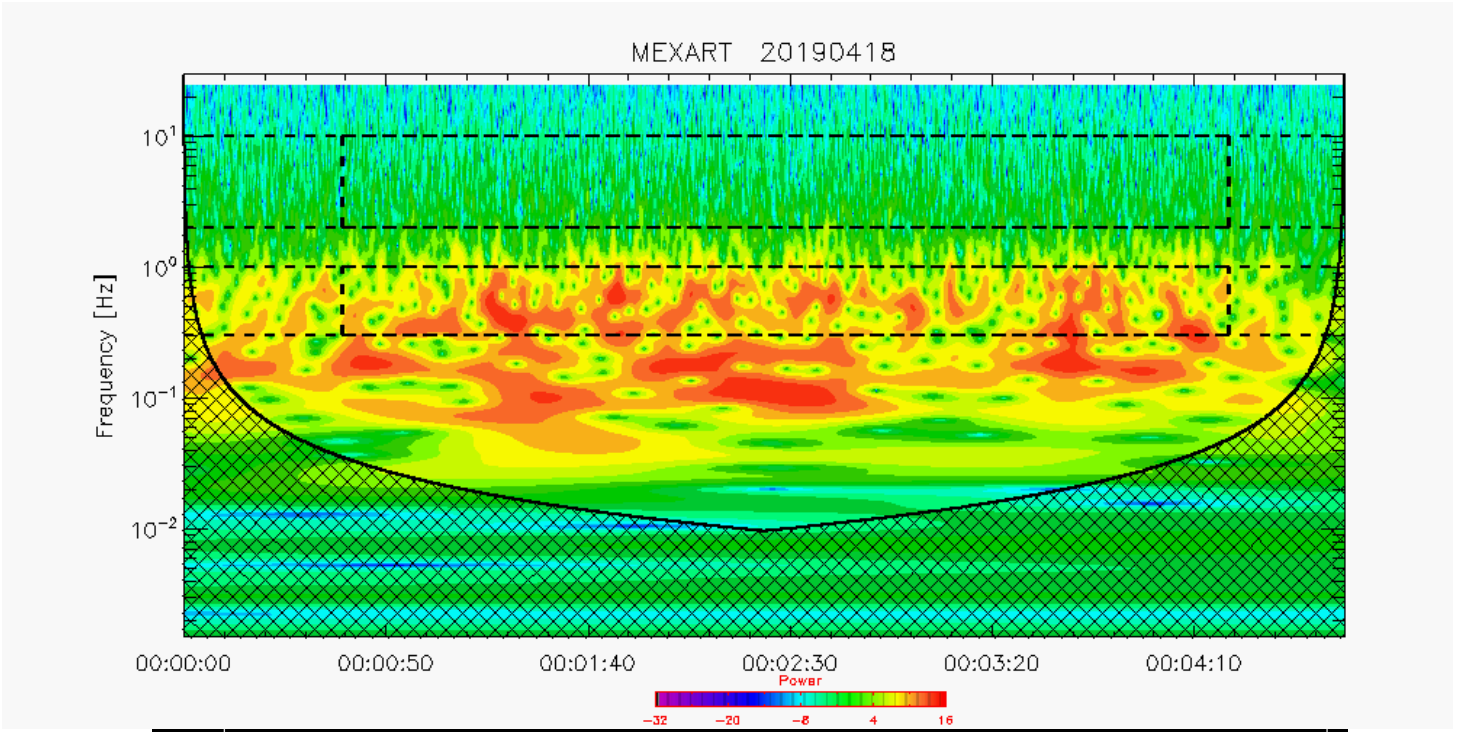
MEXART 20190418
Frequency [Hz]
10^1
10^0
10^{-1}
10^{-2}
00:00:00
00:00:50
00:01:40
00:02:30
00:03:20
00:04:10
Power
−32
−20
−8
4
16

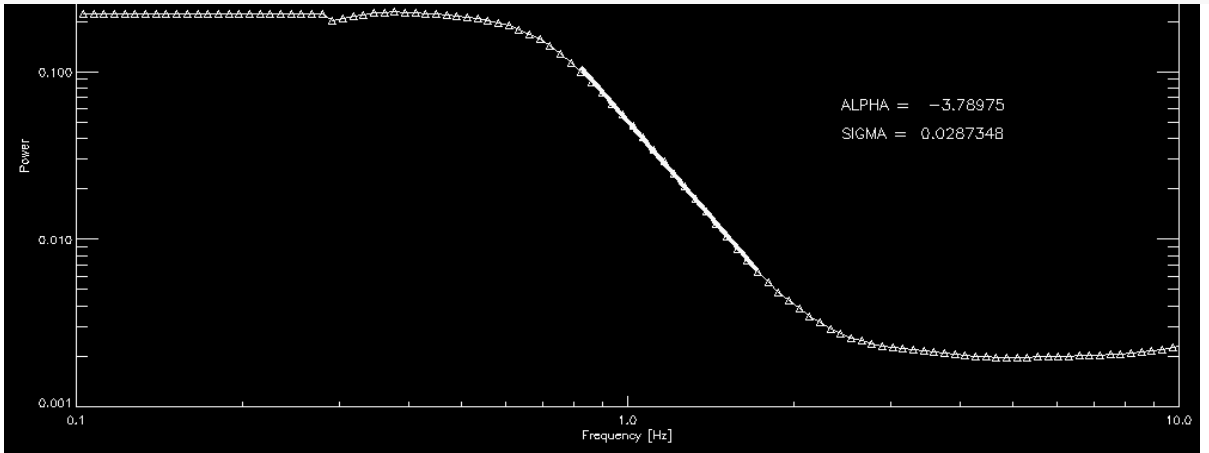
Power
0.100
0.010
0.001
0.1
1.0
10.0
Frequency [Hz]
ALPHA = −3.78975
SIGMA = 0.0287348

A New Digital Backend for the Mexican Array Radio Telescope

Alessio Magro*, Riccardo Chiello†, Denis Cutajar*, Josef Borg*, Kristian Zarb-Adami*†‡,
Americo Gonzalez-Esparza§, Julio Mejía-Ambriz§, Ernesto Aguilar-Rodriguez§ Adan Espinosa-Jimenez§
J.L. Godoy-Hernandez§ and Ernesto Andrade-Mascote§
*Institute of Space Sciences and Astronomy, Univesity of Malta, Malta
e-mail: alessio.magro@um.edu.mt, denis.cutajar@um.edu.mt, kristian.zard-adami@um.edu.mt
†Department of Astrophysics, University of Oxford, UK
e-mail: riccardo.chiello@physics.ox.ac.uk, kza@astro.ox.ac.uk
‡Osservatorio Astrofisico di Catania, INAF, Italy
§LANCE, Instituto de Geofísica, Universidad Nacional Autónoma de México
e-mail: americo@igeofisica.unam.mx, jcmejia@geofisica.unam.mx, ernesto@geofisica.unam.mx

Conclusions

The Morlet wavelet is the appropriate option because it ensures a good frequency resolution for IPS and IONS.

The WT method to obtain IPS index: <Power ips> - <Power noise> can be a alternative method to obtain in a straightforward way the m index, probably also for IONS to obtain S_4 index.

Interferences can be easily identified and eliminated by using WT using variable-sized windows.

The wavelet transform (WT) function can be used to obtain the IPS power spectra. No Fourier transform is needed.

Practically same solar wind speeds values obtained from power spectra with WT and Fourier transform.

Few works have used the WT in IPS and IONS to explore local physical parameters of the small-scale fluctuations.

The level of IONS intensity and IONS frequency is not very well identified to the nature of space weather events.

LANCE

Laboratorio Nacional
de Clima Espacial

IGUM
INSTITUTO de GEOFÍSICA
Unidad Michoacán

OBSERVATORIO DE CENTELLEO INTERPLANETARIO COENEO MICHOACÁN
MEXART

Thanks!